Palaeogeography, Palaeoclimatology, Palaeoecology 285 (2010) 1–16

Contents lists available at ScienceDirect

Palaeogeography, Palaeoclimatology, Palaeoecology

journal homepage: www.elsevier.com/locate/palaeo

Rhaetian magneto-biostratigraphy from the Southern Alps (Italy): Constraints on Triassic chronology

Giovanni Muttoni [a,b,*], Dennis V. Kent [c,d], Flavio Jadoul [a], Paul E. Olsen [d], Manuel Rigo [e], Maria Teresa Galli [a], Alda Nicora [a]

[a] Department of Earth Sciences, University of Milan, Via Mangiagalli 34, I-20133 Milan, Italy
[b] ALP — Alpine Laboratory of Paleomagnetism, via Madonna dei Boschi 76, I-12016 Peveragno (CN), Italy
[c] Earth and Planetary Sciences, Rutgers University, Piscataway, NJ 08854, U.S.A.
[d] Lamont-Doherty Earth Observatory, Palisades, NY 10964, U.S.A.
[e] Department of Geosciences, University of Padova, Via Giotto 1, 35137, Padova, Italy

ARTICLE INFO

Article history:
Received 6 October 2008
Received in revised form 14 October 2009
Accepted 14 October 2009
Available online 23 October 2009

Keywords:
Magnetostratigraphy
Biostratigraphy
Rhaetian
Triassic
Time scale

ABSTRACT

New Late Triassic–earliest Jurassic magneto-biostratigraphic data have been obtained from three overlapping sections in the Southern Alps, Italy (Costa Imagna, Brumano, Italcementi Quarry), composed of ~520 m of shallow-marine carbonates outcropping in stratigraphic continuity. Characteristic magnetic components of presumed depositional age record a sequence of 9 normal and reverse polarity magnetozones (as defined by at least three stratigraphically superposed samples) linked by conodont and palynofloral evidence from this study and the literature to Rhaetian to Triassic–Jurassic boundary age. This represents a significantly larger number of polarity zones than previously recognized in more condensed Rhaetian sections from the literature, and by inference represents more time. These data are placed in a broader Late Triassic temporal framework by means of correlations to published magneto-biostratigraphic data from the Tethyan marine Pizzo Mondello section and the Newark astronomical polarity time scale (APTS). This framework is consistent with a position of the Norian–Rhaetian boundary (as defined at Brumano and Pizzo Mondello by the first appearance of *Misikella posthernsteini*) within Newark magnetozones E17r–E19r in the ~207–210 Ma time interval, in basic agreement with the position originally estimated in the Newark using pollen biostratigraphy (E18 at 208–209 Ma). This framework is also consistent with the position of the Triassic–Jurassic boundary interval (placed at Italcementi Quarry at the acme of *Kraeuselisporites reissingeri* coincident with a negative carbon isotope excursion) correlative to just above Newark magnetozone E23r and just below the oldest CAMP lavas dated at ~202 Ma. Hence, we estimate the duration of the Rhaetian to be ~5.5–8.5 Myr (or even longer if the Triassic–Jurassic boundary is instead placed above the negative carbon isotope excursion as at Kuhjoch, which is the designated GSSP for the base of the Hettangian), and encompassing 9 magnetozones. This duration contrasts with a duration of ~2 Myr and only ~4 magnetozones in several alternative published magneto-biostratigraphic schemes.

© 2009 Elsevier B.V. All rights reserved.

1. Introduction

The Triassic is a ~50 Myr-long period of significant adaptive radiation of marine and continental life bracketed between two major extinction events, yet only three of the eight stage boundaries that define its chronostratigraphy have been thus far officially ratified by the International Commission on Stratigraphy (i.e., base Induan = base Triassic; Yin et al., 2001; base Ladinian = base Middle Triassic; Brack et al., 2005; and base Carnian = base Late Triassic; Mietto et al., 2007). Uncertainty in the demarcation and correlation of stage boundaries is reflected in a debate on the calibration of the Triassic time scale (Gradstein et al., 2004; Brack et al., 2005; Kent et al., 2006). For the Late Triassic, an astrochronology anchored to magnetostratigraphy and radiometric dates is available from the continental sections of the Newark Supergroup (Kent et al., 1995; Kent and Olsen, 1999; Olsen and Kent, 1999), whereas magnetostratigraphy is available with conodont biostratigraphy and rare radiometric dates tied to the ammonoid zonation for the Tethyan realm. The Newark continental astronomical polarity time scale (APTS) and Tethyan marine biostratigraphy can therefore be correlated using the universal record of polarity reversals for the construction of an integrated Late Triassic time scale. While fundamental steps in this direction have already been taken, the issue is not yet settled, most glaringly for the Rhaetian.

* Corresponding author. Department of Earth Sciences, University of Milan, Via Mangiagalli 34, I-20133 Milan, Italy. Fax: +39 02 503 15494.
E-mail address: giovanni.muttoni1@unimi.it (G. Muttoni).

0031-0182/$ – see front matter © 2009 Elsevier B.V. All rights reserved.
doi:10.1016/j.palaeo.2009.10.014

Two options for the duration of the Rhaetian were recently proposed using magnetostratigraphic correlation of conodont biostratigraphic data from selected Tethyan sections to the Newark APTS. According to Gallet et al. (2007 and references therein), the Rhaetian has a short duration (~2 Myr) straddling only about 3 polarity chrons, and moreover, it is supposedly in part missing in the Newark APTS (Fig. 1, left panels 'Tethyan composite I' and 'Oyuklu section'). In contrast, according to Channell et al. (2003) and Muttoni et al. (2004), the Rhaetian would represent a time of ~6–7 Myr from Newark magnetozone E17 at ~209 Ma to the Triassic–Jurassic (T–J) boundary located just

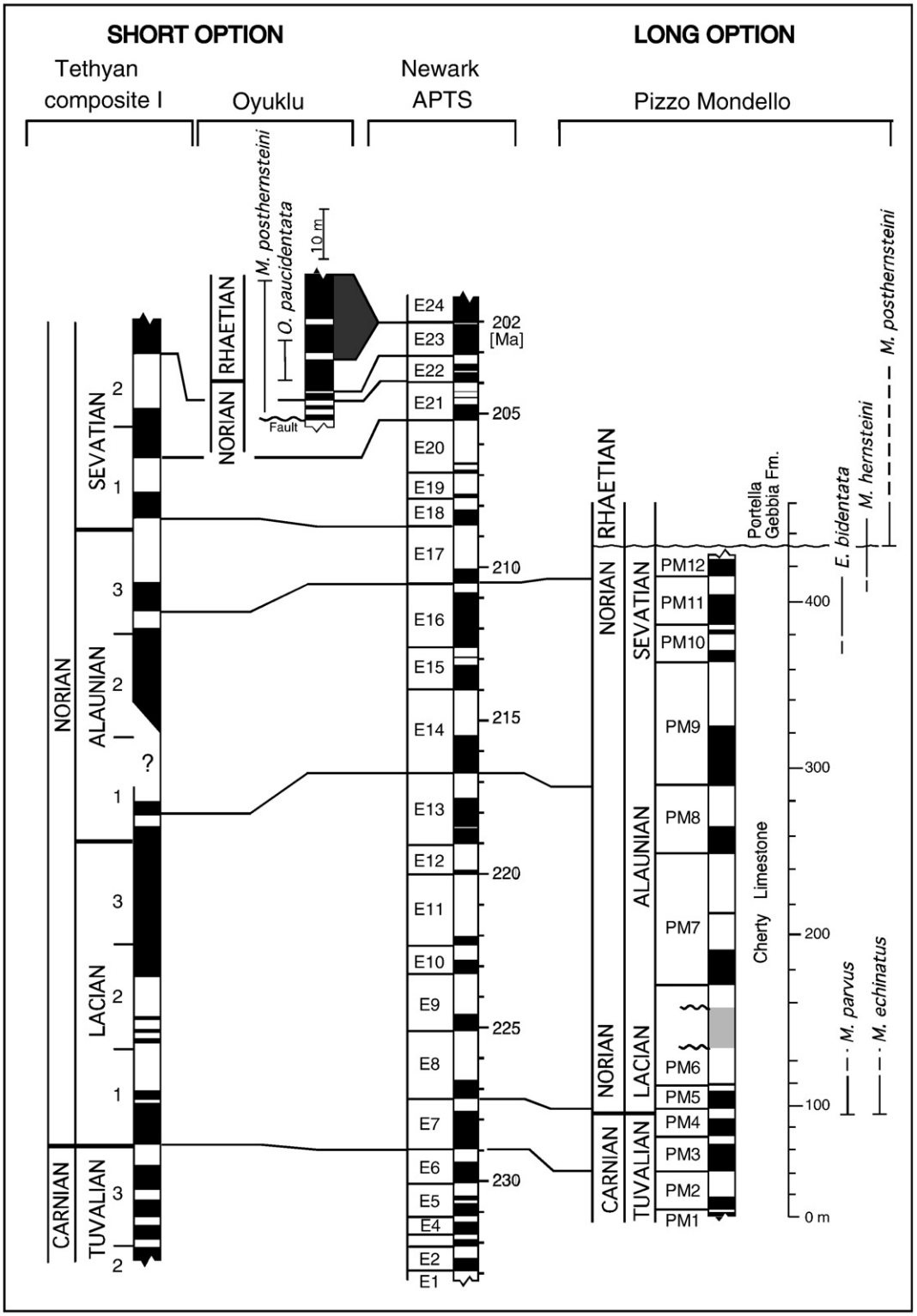

Fig. 1. Short duration vs. long duration options for the Rhaetian, the youngest stage of the Triassic. According to the compilation of magneto-biostratigraphic data from the Tethyan realm of Krystyn et al. (2002) and Gallet et al. (2003) (Tethyan composite I), and recent data from Oyuklu (Gallet et al., 2007), the Rhaetian is ~2 Myr in duration and in part missing in a supposed gap in the Newark APTS (Kent and Olsen, 1999). According to data from Pizzo Mondello (Muttoni et al., 2004), the Rhaetian should be ~6–7 Myr long, virtually similar in duration to the original estimate of Kent and Olsen (1999). The Triassic–Jurassic boundary in Newark section based on palynofloral evidence occurs near the base of E24n. See text for discussion.

above magnetozone E23r at ~202 Ma, straddling 8 to 10 polarity chrons and a duration similar to that of ~6 Myr originally proposed for the Newark section by Kent et al. (1995) and Olsen and Kent (1999) on the basis of pollen biostratigraphy (Olsen et al., 1996) (Fig. 1, right panel 'Pizzo Mondello'; Muttoni et al., 2004). In this paper, we contribute to the issue of the duration of the Rhaetian by presenting magnetostratigraphic data from a thick composite Tethyan marine section from the Southern Alps, Italy, and review the available magneto-biostratigraphic data from the literature that constrain the chronology of the Late Triassic for comparison with the recent Triassic time scale of Gradstein et al. (2004).

2. Geological setting and stratigraphy

The uppermost Triassic succession of the Lombardian Basin in the Southern Alps north of Bergamo (Fig. 2A) consists of shales of the Riva di Solto Shale (RSS) overlain by carbonates and shales of the Zu Limestone; these are in turn overlain by Hettangian micritic limestones of the Malanotte Formation and carbonate platform deposits of the Albenza Formation (formerly Conchodon Dolomite) (Galli et al., 2005; 2007; Jadoul and Galli, 2008). The Zu Limestone was traditionally subdivided into four members (Zu1–Zu4), but the youngest member (Zu4) has been recently renamed the Malanotte Formation (Galli et al., 2007) (Fig. 2B). These mainly shallow-water units were deposited at subtropical northern hemisphere paleolatitudes on the northern margin of Adria, a promontory of Africa (e.g., Muttoni et al., 2001a; Kent and Muttoni, 2003) that faced the Tethyan Ocean to the east. These units were buried mainly under deep-water marine sediments in the Jurassic and Cretaceous, and folded and thrusted to the south by the Adria-Europe (Alpine) collision in the Cenozoic (e.g., Doglioni and Bosellini, 1987).

We studied three partially overlapping and virtually fully exposed sections, namely the ~48 m thick Costa Imagna section, the ~427 m thick Brumano section (subdivided into a 157 m thick lower Brumano section and a 270 m thick upper Brumano section), and the ~160 m thick Italcementi Quarry section. These sections crop out in close contiguity in the Southern Alps north of Bergamo and cover a ~520 m thick composite stratigraphic interval from the Zu1 member of the Zu Limestone to the base of the Albenza Formation (Fig. 2A and B). The Costa Imagna section and the lower Brumano section straddle the Zu1 member up to the boundary with the overlying Zu2 member and have been correlated by tracing laterally lithostratigraphic marker beds (Fig. 3). In general, the Zu1 member consists of monotonous alternations of dark-grey marl and marly limestone horizons intercalated with predominately thin-bedded fine-grained limestones. The lithofacies are arranged vertically into asymmetrical to nearly symmetrical, decameter-scale cycles. The upper Brumano section continues into the Zu2 member, composed of decameter-scale carbonate cycles with bioturbated or fossiliferous dark-grey wackestones or coral patch reefs at the base, and intrabioclastic and/or oolitic packstones–grainstones at the top (Fig. 3). The Zu3 member encompasses three subunits (Zu3a–c), two of which are present in the upper Brumano section (Zu3a–b) (Fig. 3). The lower subunit (Zu3a) consists of 7.5 to 15 m thick marl and micritic limestone cycles occasionally capped by thin iron-oxide crusts. The middle subunit (Zu3b) is represented by 4 to 9 m thick marl and marly limestone cycles with frequent iron-oxide thin crusts at each cycle top.

The Italcementi Quarry section straddles the Zu3b subunit and continues into the overlying Zu3c subunit (Fig. 4), consisting of 40–50 m thick bioturbated wackestones and packstones with benthic foraminifers, bivalves, crinoids, gastropods, calcisponge, ostracods, corals, and dasycladacean algae. The Zu3c subunit is overlain by the Malanotte Formation, composed of thinly bedded micritic limestones, marls and biocalcarenites progressively increasing in abundance toward the section top.

A few hundred meters to the SE of the Italcementi Quarry section is a section called Malanotte. At its base is a ~1 m thick horizon of marlstones–siltstones characterized by a marked negative carbon isotope excursion with minimum values of ~−1‰ followed across much of the overlying part of the Malanotte Formation by an extended positive excursion with maximum values of ~4‰ and by a second negative peak with a minimum value of around 2‰ (Galli et al., 2005; 2007) (Fig. 4). At the Italcementi Quarry section, correlated to the nearby Malanotte section by means of detailed

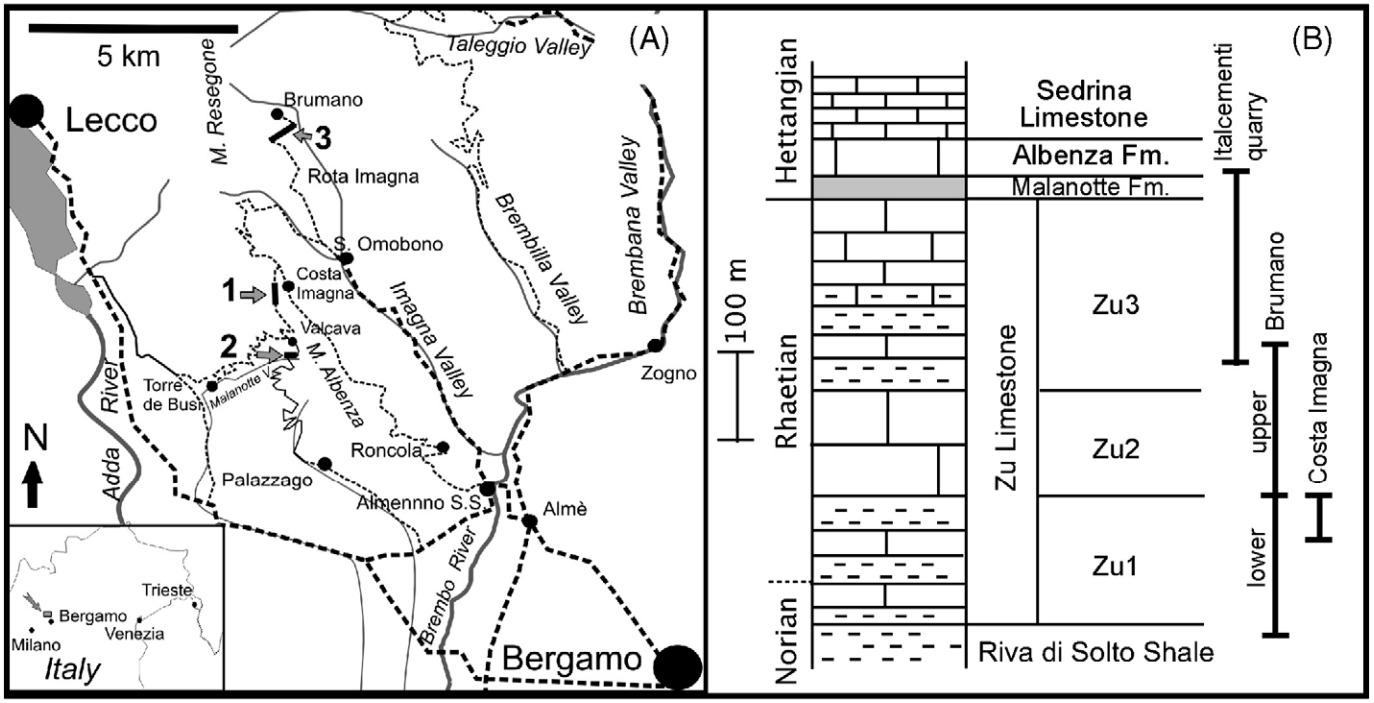

Fig. 2. (A) Location map of the sampling area with indication of sampling sections (1 = Costa Imagna; 2 = Italcementi Quarry and Malanotte; 3 = Brumano lower and upper sections). (B) Stratigraphy of the sampled interval with indication of stratigraphic coverage of individual sections.

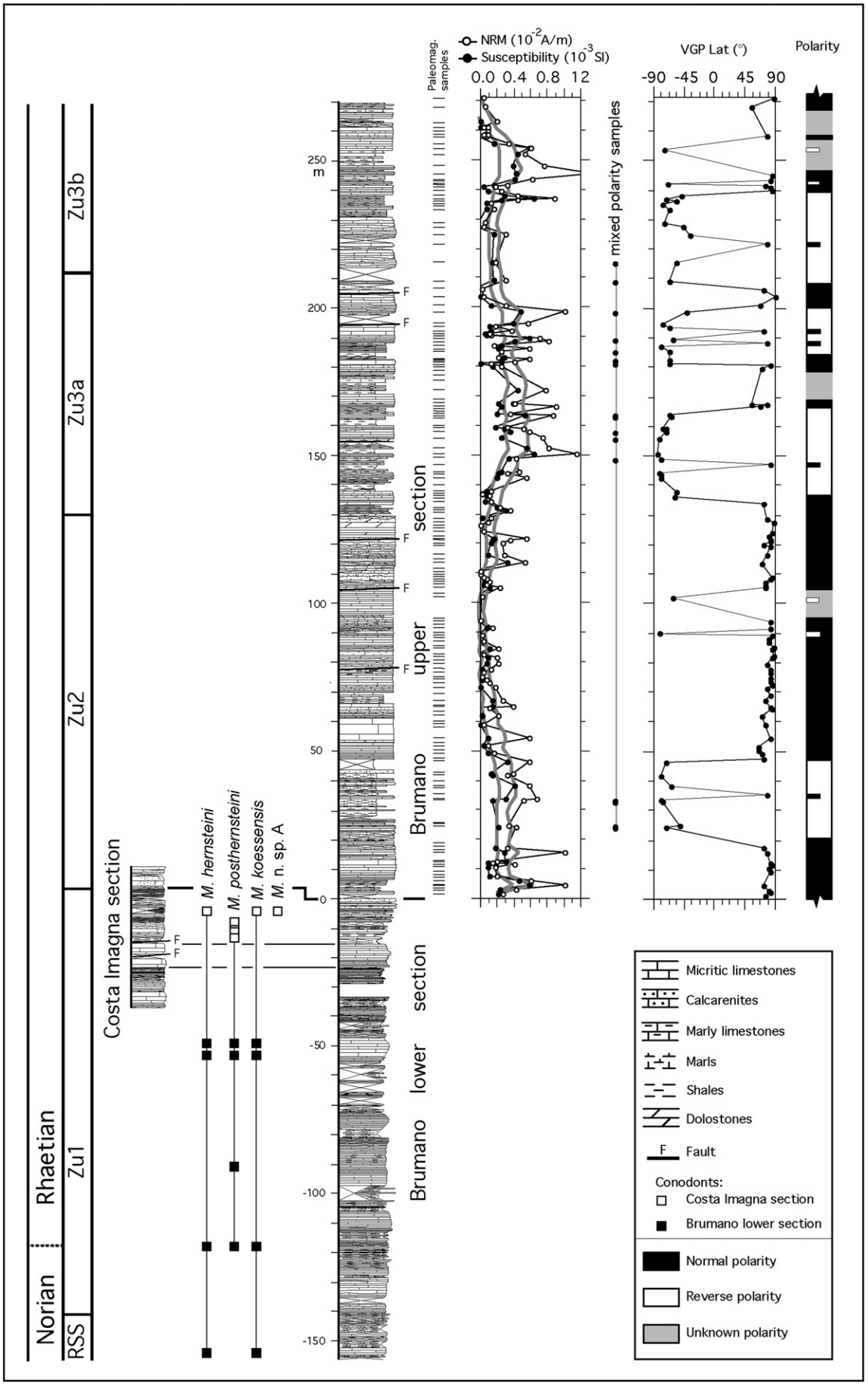
Norian
Rhaetian
RSS
Zu1
Zu2
Zu3a
Zu3b
Costa Imagna section
M. hernsteini
M. posthernsteini
M. koessensis
M. n. sp. A
Brumano lower section
Brumano upper section
Paleomag. samples
NRM (10-2A/m)
Susceptibility (10-3SI)
0.0 0.4 0.8 12
mixed polarity samples
VGP Lat (°)
-90 -45 0 45 90
Polarity
250
m
200
150
100
50
0
-50
-100
-150
F
Micritic limestones
Calcarenites
Marly limestones
Marls
Shales
Dolostones
Fault
Conodonts:
Costa Imagna section
Brumano lower section
Normal polarity
Reverse polarity
Unknown polarity

lithostratigraphy (Galli et al., 2005; 2007), this marlstone–siltstone level and the associated initial negative carbon isotope excursion are absent, and the base of the Malanotte Formation lies directly on top of the Zu3c subunit by way of a mm thick iron-rich hardground (Galli et al., 2005; 2007) (Fig. 4).

3. Biostratigraphy

Triassic stages have been historically based on ammonoids, but because they are very rare, other more common taxa such as conodonts have been widely used for the recognition of Triassic stages (Figs. 5 and 6), and we use them here. We sampled for conodonts throughout the Zu1–Zu3 interval at Costa Imagna and Brumano. Conodonts were found in the lower Brumano section and in the Costa Imagna section (Figs. 3 and 6), whereas the upper Brumano section and the Italcementi Quarry section have not yet produced conodonts.

The lower Brumano section contains specimens of *Misikella posthernsteini* Kozur and Mock and *Misikella hernsteini* (Mostler). In the upper part of the lower Brumano section, *Misikella koessenensis* also occurs (Figs. 3 and 6). The Costa Imagna section yielded a conodont fauna mainly composed of the species *M. posthernsteini*, *M. hernsteini*, and *Misikella* n. sp. A (Figs. 3 and 6), in association with ramiform elements. The joint occurrence of *M. posthernsteini* and *M. hernsteini* characterizes the *M. hernsteini–M. posthernsteini* Subzone, which represents the lower part of the *M. posthernsteini* Assemblage Zone (Kozur and Mock, 1991) (Fig. 5). The stratigraphic range of the *M. hernsteini–M. posthernsteini* Subzone is correlative to the *Paracochloceras suessi* and *'Choristoceras' haueri* Tethyan ammonoid Zones of Krystyn (1987; 1990). According to Kozur and Mock (1991), the base of the *M. hernsteini–M. posthernsteini* Subzone corresponds to the base of the Rhaetian (Fig. 5). Recently, Krystyn et al. (2007a) proposed two options for the base of the Rhaetian using conodonts at Steinbergkogel, namely the first occurrence of *M. hernsteini* or, 0.4 m above, the first appearance of *M. posthernsteini*.

The stratigraphic interval straddling the uppermost Zu3c member and the overlying Malanotte Formation at the Italcementi Quarry and Malanotte sections, as well as at several other correlative sections in the Lombardian Basin, contains palynological evidence for the T–J boundary. At the most continuous Malanotte section, the boundary was placed within the ~1 m thick marly–silty horizon and the base of the Malanotte Formation, characterized by a marked negative carbon isotope excursion (Fig. 4, upper left panel, excursion '1'), between the disappearance of Rhaetian pollens such as *Rhaetipollis germanicus* that are typical of the Zu3c member, and an acme of *Kraeuselisporites reissingeri* associated with other diagnostic Hettangian pollens typical of the Malanotte Formation (i.e., *Classopollis torosus*, *Gliscopollis meyeriana*, *Microreticulatisporites fuscus*, *Callialasporites* spp., *Retitriletes austroclavatidites*, *R. clavatoides*, *Tsugapollenites pseudomassulae*, and rare occurrences of *Cerebropollenites macroverrucosus*; Galli et al., 2005; 2007). As previously pointed out, this basal ~1 m thick marly–silty horizon is absent at the Italcementi Quarry section, albeit the general distribution of the T–J boundary pollen taxa has been also recognized therein (Galli et al., 2005; 2007) (Fig. 4).

Galli et al. (2005) pointed out that the rich and diversified benthic foraminiferal assemblages, the reef communities, and other reef-associated organisms disappear at the top of the Zu Limestone and argued that this biotic crisis represents the local expression of the globally identified end-Triassic extinction event. In the Malanotte section, as well at several other correlative sections in the Lombardian Basin, the marine extinction at the top of the Zu Limestone coincides with the onset of the basal negative carbon isotope excursion (Fig. 4, upper left panel, excursion '1') and with a shallow-water productivity crisis (Galli et al., 2005).

Recently, the proposal of Hillebrandt et al. (2007) to place the GSSP for the base of the Hettangian and hence the T–J boundary at the first occurrence of the ammonite *Psiloceras spelae* at the Kuhjoch section in Austria was accepted by vote of the members of the Triassic–Jurassic Boundary Working Group of the International Subcommission on Jurassic Stratigraphy (Morton, 2008a, 2008b; Morton et al., 2008). At Kuhjoch, the first occurrence of *P. spelae* occurs ~6 m above a negative carbon isotope excursion located across the lithological boundary between the Kössen Formation (Eiberg Member) and the Kendelbach Formation (Tiefengraben Member); *Rhaetipollis germanicus* disappears ~1 m above this negative carbon isotope excursion (in the lower part of the Schattwald Beds of the Tiefengraben member). The Kuhjoch negative carbon isotope excursion should therefore correspond (within available stratigraphic resolution of ~1 m or less) to the basal negative excursion '1' observed at the base of the Malanotte Formation, which is also closely associated with the disappearance of *R. germanicus* (Fig. 4). The interval between the base of the isotopic excursion and the last occurrence of *R. germanicus* also overlaps the last occurrences of conodonts at other localities, and Triassic-aspect ammonites, notably *Choristoceras*. Hence, considering the base of the Rhaetian at the first appearance of *Misikella posthernsteini*, which is provisionally placed near the base of the Brumano lower section (Fig. 3), and the end-Triassic extinction interval, placed at the negative carbon isotope excursion at the base of the Malanotte Formation in the Malanotte section (which predates by a yet unknown amount of time the first occurrence of *P. spelae*, not found at Italcementi Quarry), we conclude that the Rhaetian in this sector of the Southern Alps corresponds to at least 490 m of shallow-marine strata.

4. Paleomagnetism

Paleomagnetic samples were drilled and oriented in the field at a nominal sampling interval of ~1.2–1.5 m giving a total of 175 standard ~11 cm^3 specimens in the upper Brumano section (Fig. 3) and 162 specimens in the Italcementi Quarry section (Fig. 4); pilot sampling in the lower Brumano section (Fig. 3) revealed unstable paleomagnetic properties and further work was not continued there. The intensity of the natural remanent magnetization (NRM), measured on a 2G DC-SQUID cryogenic magnetometer housed in a magnetically shielded room, showed at Brumano decameter-scale variations around a mean value of 3 mA/m, with lower values (~1.5 m/Am) in the highly calcareous Zu2 member, and higher values (~5 m/Am) in the more marly Zu3a and Zu3b subunits (Fig. 3). The initial susceptibility follows the NRM intensity trends suggesting dominant control by variations in amount and/or type of magnetic mineral(s) rather than in Earth's magnetic field intensity at the time of NRM acquisition. At the Italcementi Quarry section, the average NRM intensity is ~0.7 mA/m, i.e. one order of magnitude lower than at Brumano, and the initial susceptibilities are also very low or even in the diamagnetic (negative) range. Because of these relatively low NRM intensities and susceptibilities, an isothermal remanent magnetization (IRM) of 0.2 T was imparted to 58 rock samples to check on variations in magnetic properties. IRM intensity oscillations around a mean value of 0.2 10^{-4} Am^2/kg are observed, with lithologically controlled decameter-scale cyclicity similar to that observed at Brumano (Fig. 4).

Fig. 3. Composite log comprising the Brumano lower section, Brumano upper section, and Costa Imagna section. The Costa Imagna section was correlated to the Brumano lower section using several laterally continuous marker beds (examples given by thin horizontal lines on figure). From left to the right: lithology subdivisions and biostratigraphic age attribution, stratigraphic positions of paleomagnetic samples, natural remanent magnetization (NRM) and initial susceptibility, latitude of the sample VGP relative to the north pole of the mean paleomagnetic axis, with magnetic polarity zones shown by filled (open) bars for normal (reverse) polarity. The position of mixed polarity samples is indicated. RSS is Riva di Solto Shale. See text for discussion.

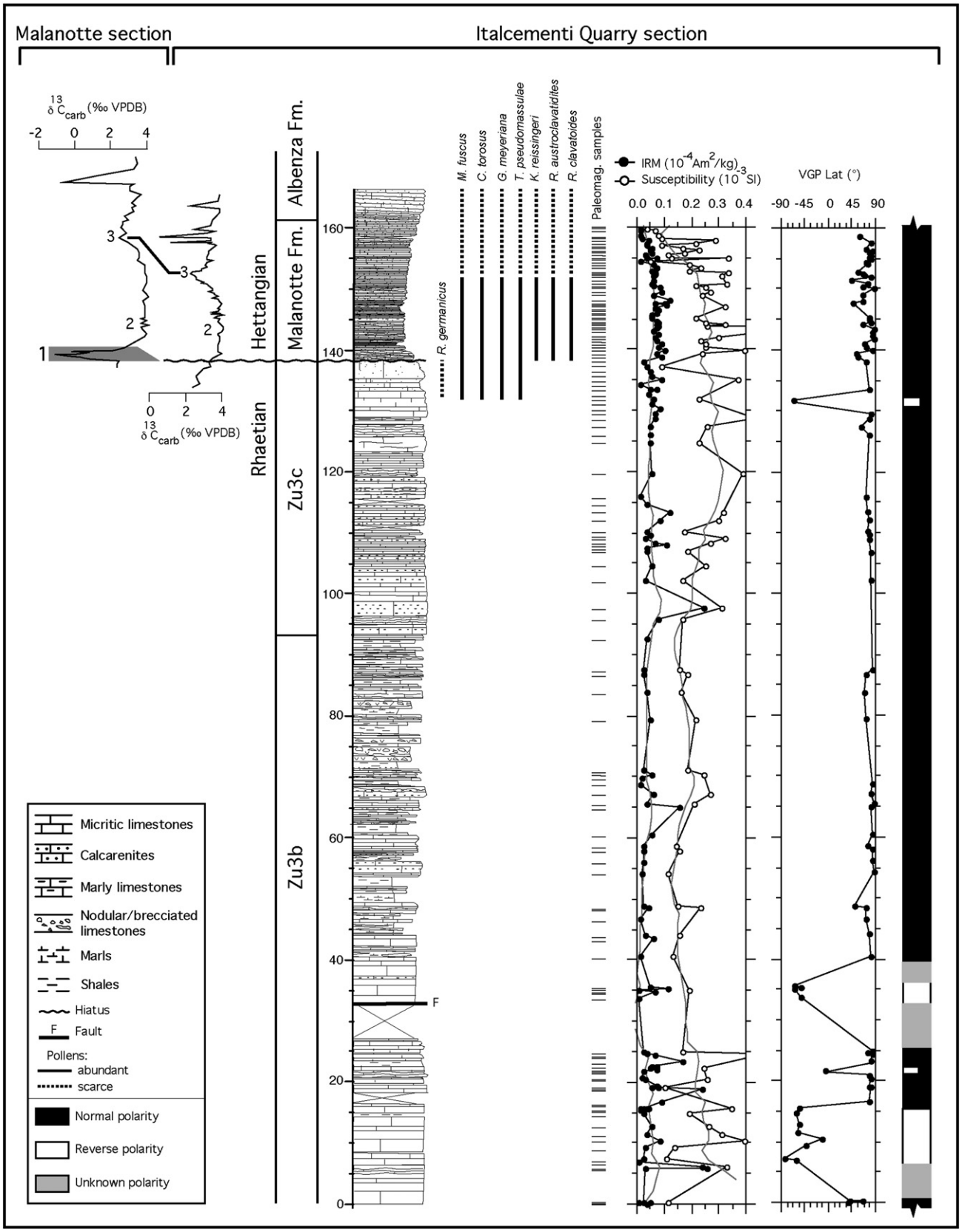

Fig. 4. Italcementi Quarry section. From left to the right: lithology subdivisions, ranges of palynomorph taxa and biostratigraphic age attribution, stratigraphic positions of paleomagnetic samples, natural remanent magnetization (NRM) and isothermal remanent magnetization (IRM), latitude of the sample VGP relative to the north pole of the mean paleomagnetic axis, with magnetic polarity zones shown by filled (open) bars for normal (reverse) polarity. Panels on the upper left side are the carbon isotope profiles from Italcementi Quarry and the nearby Malanotte section across the Triassic–Jurassic boundary (Galli et al., 2005; 2007). See text for discussion.

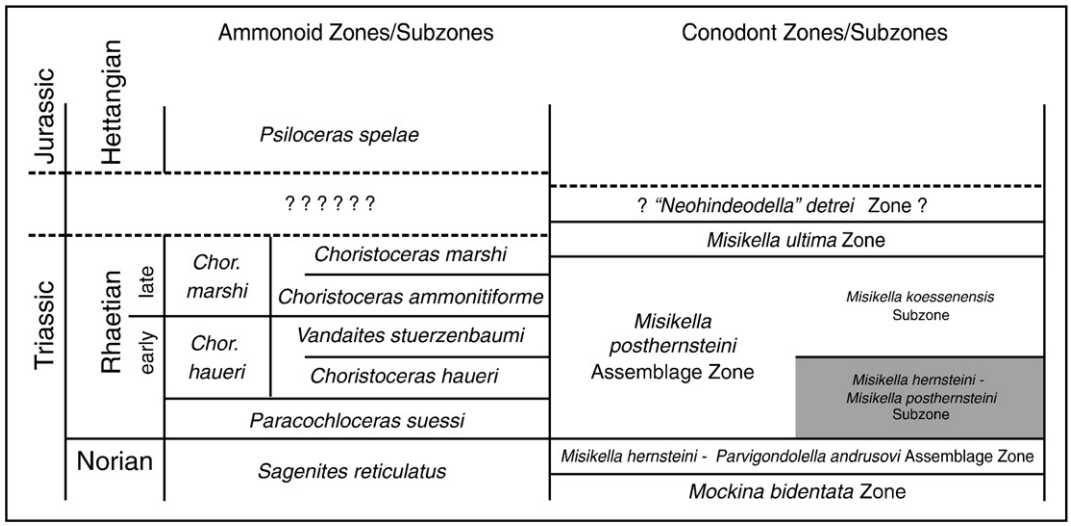

Fig. 5. Late Norian–Hettangian ammonoid and conodont zonation (after Krystyn, 1987; 1990; Kozur and Mock, 1991). The conodont zonation proposed by Kozur and Mock (1991) has been here modified by attributing an early Jurassic age to the *Neohindeodella detrei* Zone (after Pálfy et al., 2007). The upper part of the Zu1 member belongs to the conodont *Misikella hernsteini–Misikella posthernsteini* Subzone (lower Rhaetian), marked by the grey area. Ammonoid and conodont zonations are not on a linear time axis.

A representative suite of samples from Brumano and Italcementi Quarry was subjected to rock-magnetic analysis using IRM backfield acquisition curves (up to 2.5 T) and thermal decay of a three component IRM (Lowrie, 1990) acquired along sample orthogonal axes in 2.5 T (high), 0.4 T (medium), and 0.12 T (low) fields (Fig. 7). Two types of IRM acquisition curves were observed: (i) IRM increased steeply resulting in a relatively low coercivity of remanence (Bcr) of less than 0.1 T, then it continued to climb, reaching a plateau from ~0.4–0.5 T up to 2.5 T field (Fig. 7A and B); this response is interpreted as resulting from the presence of a dominant low-medium coercivity mineral. (ii) IRM increased steeply as in case (i), reached an apparent plateau but subsequently it continued to climb gently with no tendency to saturate even in a field of 2.5 T; this response is interpreted as resulting from the coexistence of low-medium and high coercivity minerals. The thermal decay of a three component IRM shows that samples are dominated by the low-medium coercivity component with maximum unblocking temperatures in the order of 500–550 °C (Fig. 7C and D). The high coercivity component is generally a very small fraction of the total remanence; when better expressed, it shows an occasional initial drop in intensity between room temperature and 100 °C, and maximum unblocking temperatures that persist above 570 °C. These observations suggest that the analyzed samples are dominated by a low-moderate coercivity magnetite phase coexisting with minor amounts of high coercivity phases such as goethite and hematite.

Samples were thermally demagnetized from room temperature up to a maximum of 570 °C adopting 50 °C steps or 25–10 °C steps close to critical unblocking temperatures. The component structure of the NRM was monitored after each demagnetization step by means of vector end-point demagnetization diagrams. Magnetic components were calculated by standard least-square analysis on linear portions of the demagnetization paths and plotted on equal-area projections for standard Fisher statistics calculation.

An initial (low temperature) A component was observed in 83% of the Brumano samples (overall mean declination, $D = 356.5°$, inclination, $I = 61.2°$, radius of 95% confidence circle, $\alpha_{95} = 1.5°$, number of component vectors, $N = 145$) and in 73% of the Italcementi Quarry samples ($D = 4.4°$E, $I = 62.3°$, $\alpha_{95} = 2.8°$, $N = 118$). This A component was isolated in the demagnetization window between ~100 °C and 200–250 °C and is interpreted as a viscous overprint possibly associated with recent weathering since the overall mean direction is broadly aligned in *in situ* coordinates along the recent geocentric axial dipole (GAD) field direction ($I = 64°$) (Figs. 8 and 9; Table 1). Removal of this A component revealed the presence of a bipolar characteristic C component oriented northerly-and-down or southerly-and-up and trending to the origin of the demagnetization axes in 66% of the Brumano samples and in 57% of the Italcementi Quarry samples. This C component was usually isolated in the demagnetization window between ~350 °C and ~500 °C at Brumano, or ~300 °C and ~475 °C at Italcementi Quarry, and is characterized by overall mean angular deviation (MAD) values of $4° \pm 3°$ and $6° \pm 5°$ at Brumano and Italcementi Quarry, respectively. Maximum unblocking temperatures approaching ~570 °C confirm the rock-magnetic data in pointing to magnetite as the main magnetic carrier in the grey limestones of the studied sections. In some samples from marl-rich intervals characterized by relatively high NRM or IRM values, such as subunit Zu3a at Brumano, the southerly-and-up C component is followed at higher unblocking temperatures by an ill-defined, down-pointing component (Fig. 8, sample B17; Fig. 3). We tentatively consider as the C component (and therefore retain for subsequent polarity interpretation) the reverse polarity portion of this mixed polarity association, and speculate that the associated normal polarity component (excluded from further analysis) is an extension to higher temperatures of the A component overprint.

The characteristic C magnetization components depart from antipodality in tilt corrected coordinates by ~26° at Brumano and ~34.5° at Italcementi Quarry (Fig. 9; Table 1). This non-antipodality is attributed to residual contamination of the reverse polarity components from the lower unblocking temperature normal polarity A component. The overall mean C component directions from both sections are $22° \pm 5°$ apart in *in situ* coordinates and $12° \pm 5°$ after bedding tilt correction. To better constrain the age of the C magnetizations, we calculated the overall mean C paleomagnetic poles from Brumano and Italcementi Quarry (Tab. 1) and compared them to the Triassic–Early Jurassic portion of the apparent polar wander (APW) path for NW Africa–Adria of Muttoni et al. (2001a) (Fig. 10, entries #1 and #2). The Italcementi Quarry paleopole in tilt corrected coordinates (Fig. 10, Italcementi) falls on the African APW path but it is somewhat removed from the Late Triassic–Early Jurassic African paleopole (entry #2) by $8° \pm 6°$ essentially in the far side direction of the sampling site. This is possibly due to inclination shallowing, which is typical of detrital (i.e. primary) magnetic grains (e.g., hematite) that may display magnetic inclinations that are shallower compared to the external geomagnetic field direction (Tauxe and Kent, 2004). The C component paleopole from Brumano falls at a similar latitude as the Italcementi paleopole (again possibly because of inclination shallowing) but it appears

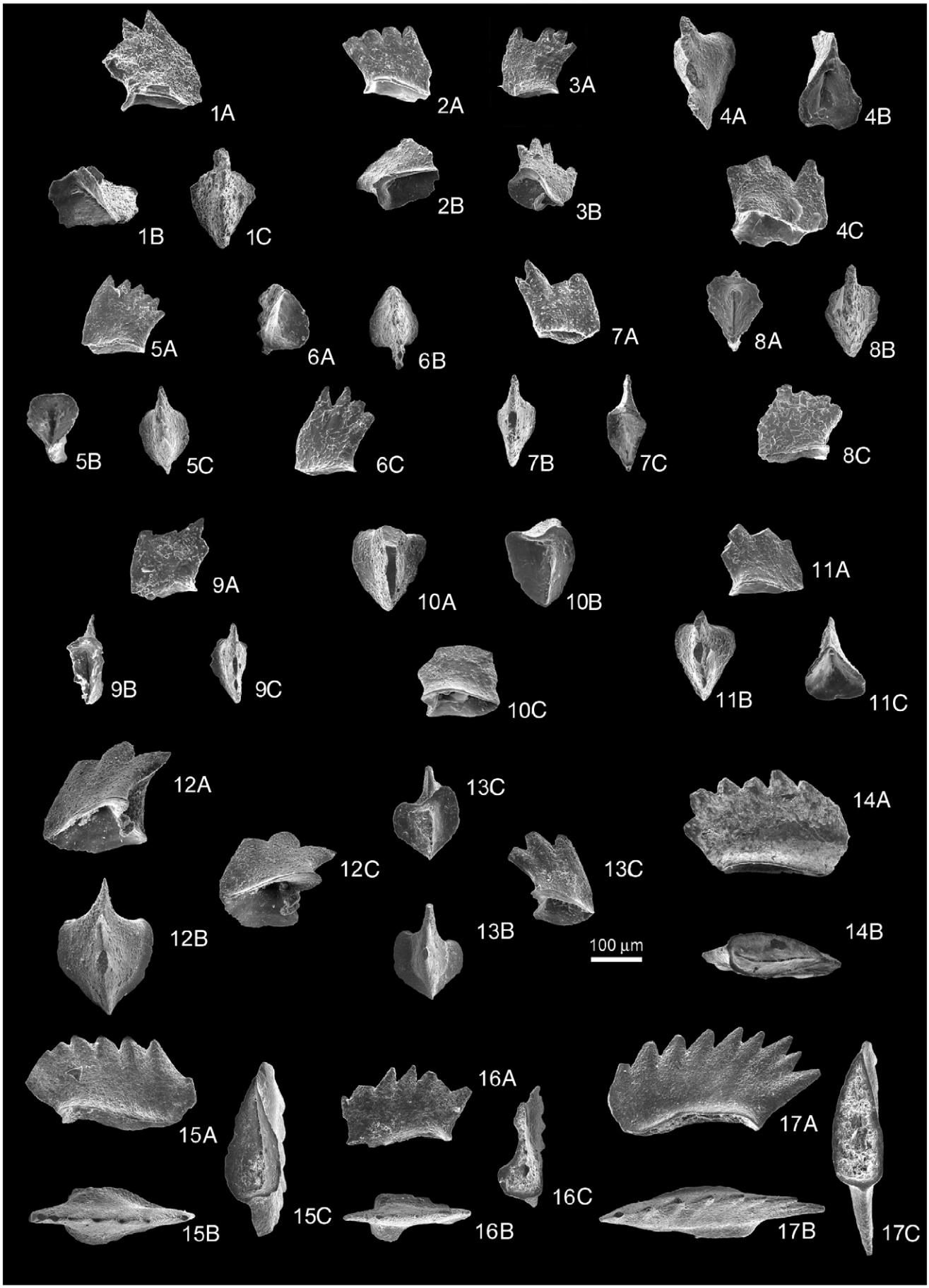
1A
2A
3A
4A
4B
1B
1C
2B
3B
4C
5A
6A
6B
7A
8A
8B
5B
5C
6C
7B
7C
8C
9A
10A
10B
11A
9B
9C
10C
11B
11C
12A
13C
14A
12C
13C
12B
13B
100 µm
14B
15A
16A
17A
15B
15C
16B
16C
17B
17C

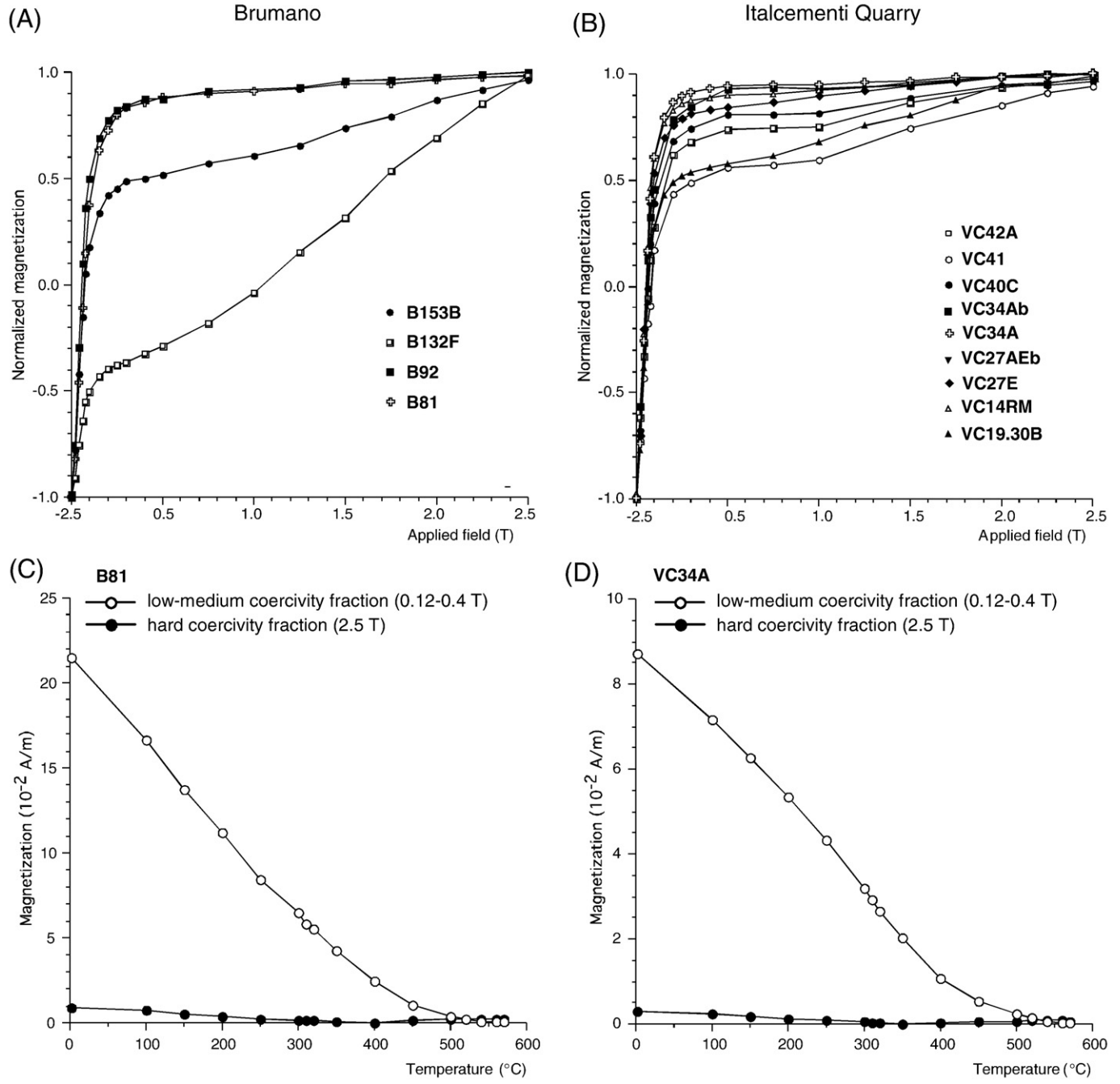

Fig. 7. Basic rock-magnetic properties using isothermal remanent magnetization (IRM) acquisition curves for Brumano (A) and Italcementi Quarry (B) samples. Thermal decay of 3-component IRM for a representative sample from Brumano (C) and Italcementi Quarry (D) indicating that samples have a dominant magnetite phase.

rotated clockwise with respect to the Late Triassic–Early Jurassic African paleopole, perhaps because of post-depositional tectonic rotations of thrust sheets during Alpine deformation in the Cenozoic since Brumano is located close to a major Alpine thrust. From these observations, we tentatively propose that the northerly-and-down and southerly-and-up C components are primary magnetizations associated with detrital magnetic particles affected by inclination shallowing that recorded a sequence of Late Triassic normal or reverse

Fig. 6. SEM micrographs of conodonts from the Zu1 member of the Zu Limestone from the Brumano lower section (BL) and the Costa Imagna section (CI). 1A. lateral view, B. lower view, C. upper view) *Misikella koessenensis* Mostler, BL, sample J 282; 2A. lateral view, B. lower view) *Misikella hernsteini* (Mostler), BL, sample J 282; 3A. lateral view, B. lower view) *Misikella koessenensis* Mostler, BL, sample J 279; 4A. upper view, B. lower view, B. lateral view) *Misikella posthernsteini*? Kozur and Mock, BL, sample J 279; 5A. lateral view, B. lower view, C. upper view) *Misikella koessenensis* Mostler, 1974, BL, sample J 270; 6A. lower view, B. upper view, C. lateral view) transitional form *Misikella hernsteini*/*posthernsteini*, BL, sample J 269; 7A. lateral view, B. upper view, C. lower view) *Misikella koessenensis* Mostler, BL, sample J 270; 8A. lower view, B. upper view, C. lateral view) *Misikella posthernsteini* Kozur and Mock, BL, sample J 269; 9A. lateral view, B. lower view, C. upper view) *Misikella koessenensis* Mostler, BL, sample J 270; 10A. upper view, B. lower view, C. lateral view) *Misikella posthernsteini* Kozur and Mock, BL, sample J 276; 11A. lateral view, B. upper view, C. lower view) *Misikella posthernsteini* Kozur and Mock, BL, sample J 279; 12A. lateral/lower view, B. upper view, C. lower view) *Misikella posthernsteini* Kozur and Mock, CI, sample J 22a; 13A. lower view, B. upper view, C. lateral view) *Misikella posthernsteini* Kozur and Mock, CI, sample J 22a; 14A. lateral view, B. lower view) *Misikella hernsteini* (Mostler), CI, sample J 18c; 15 A. lateral view, B. upper view, C. lower view) *Misikella hernsteini* (Mostler), CI, sample J 18c; 16 A. lateral view, B. upper view, C. lower view) *Misikella hernsteini* (Mostler), CI, sample J 18c; 17A. lateral view, B. upper view, C. lower view) *Misikella* n. sp. A, CI, sample J 18c. The Color Alteration Index (CAI) is 3 for BL and 2 for CI.

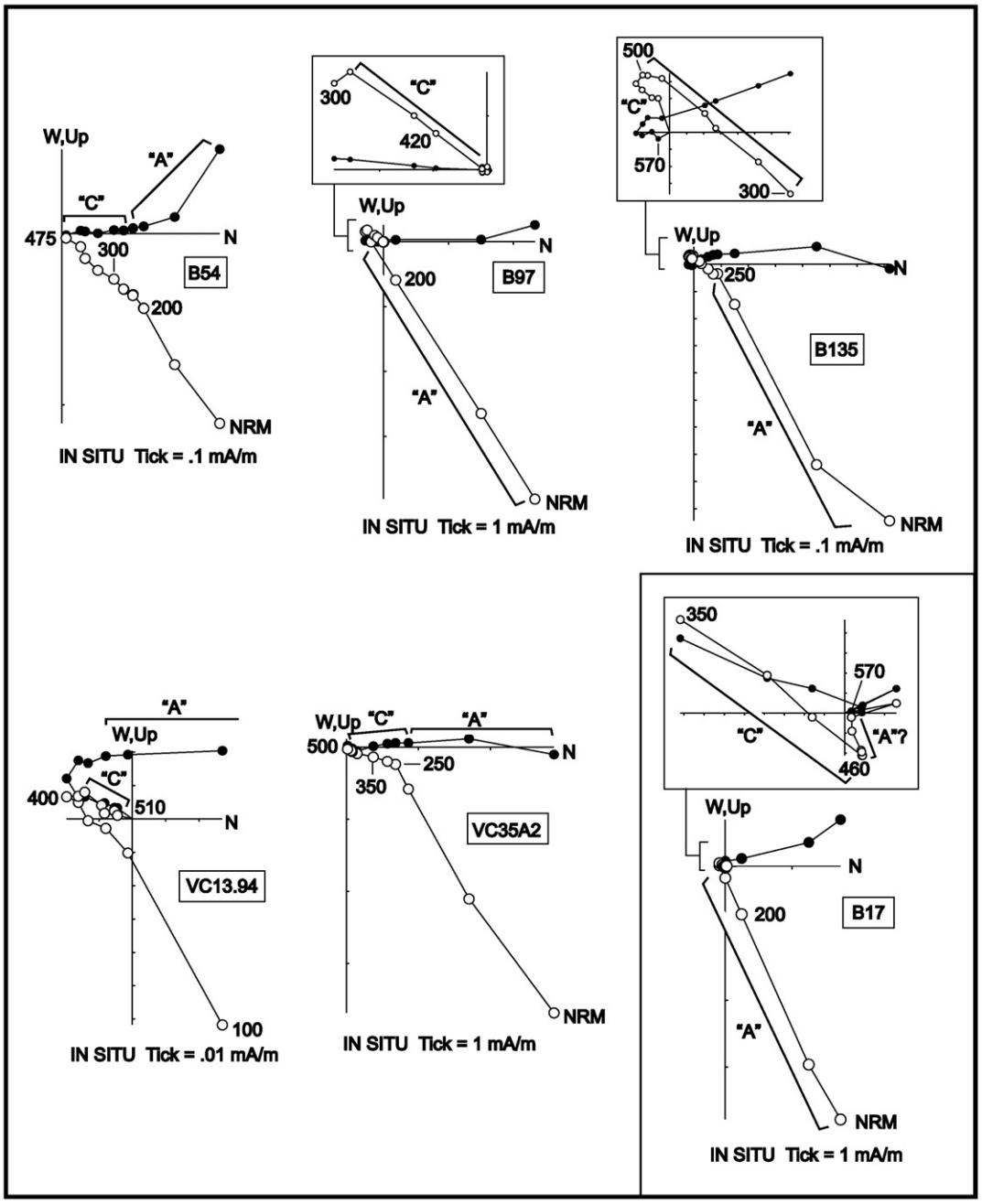

Fig. 8. Vector end-point demagnetization diagrams of representative samples from Italcementi Quarry (VC13.95 and VC35A2) and Brumano (B97 and B135) with indication of magnetic components isolated (A, characteristic C); B17 from Brumano is an example of a mixed polarity component association (see text for discussion). Closed symbols are projections onto the horizontal plane and open symbols onto the vertical plane in geographic (*in situ*) coordinates. Demagnetization temperatures are expressed in °C.

geomagnetic field polarity, respectively, at places partly masked and distorted by a complex pattern of normal polarity overprinting.

5. Magnetostratigraphy and age model

The latitude of each C component virtual geomagnetic pole (VGP) relative to the mean paleomagnetic (north) pole axis was used for interpreting polarity stratigraphy (Kent et al., 1995). VGP relative latitudes approaching +90° (north pole) or −90° (south pole) were interpreted as recording normal or reverse polarity, respectively. The Brumano section is characterized by a sequence of nine main polarity magnetozones (Fig. 3). The largely younger Italcementi Quarry section is characterized by a thick normal polarity magnetozone containing at the base two reverse polarity magnetozones (Fig. 4).

We correlate the Brumano and Italcementi Quarry sections by means of lithostratigraphy with constraints from magnetostratigraphy (Fig. 11). From field relationships, we hypothesize that the two sections overlap by some tens of meters essentially in the Zu3b subunit. The expected overlap interval straddles a broadly correlative sequence of polarity magnetozones that is however affected by faulting at both sections (Fig. 11). If we accept this broad correlation, the composite polarity sequence extends from basal normal polarity magnetozone BIT1n (where BIT is the acronym for Brumano–Italcementi) in the Rhaetian Zu2 member up to normal polarity magnetozone BIT5n extending immediately above the palynological and geochemical Triassic–Jurassic boundary interval in the Malanotte Formation (Fig. 11). The stratigraphic continuity of the polarity sequence within individual sections is maintained by the optimal

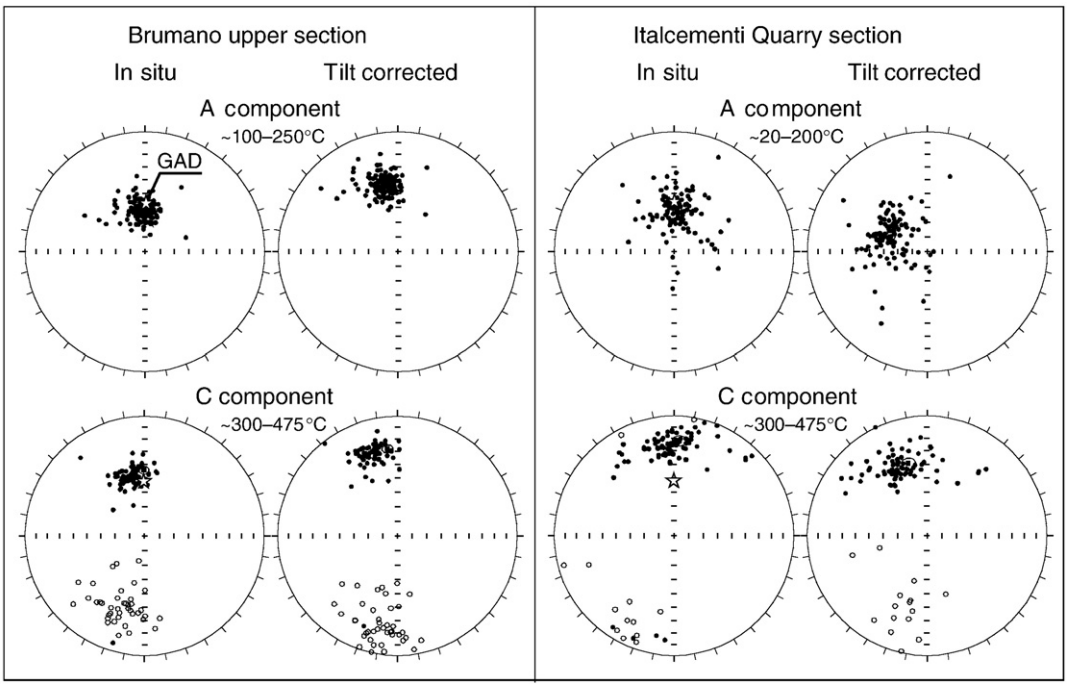

Fig. 9. Equal-area projections before (*in situ*) and after bedding tilt correction of the A and characteristic C component directions from Brumano and Italcementi Quarry (see Table 1). Closed symbols are projections onto the lower hemisphere and open symbols onto the upper hemisphere.

conditions of exposure, albeit faults with meter scale displacements have been occasionally observed throughout the sequence (Fig. 11).

We place our Rhaetian magneto-biostratigraphy in a broader Late Triassic temporal framework by means of correlations to the younger part of the Newark APTS from magnetozone E17n to E24n (Kent et al., 1995; Kent and Olsen, 1999; Olsen and Kent, 1999), which has been recently extended in the Hartford Basin to magnetozones H24–H26 (Kent and Olsen, 2008) (Fig. 11). As a possibility, Brumano–Italcementi Quarry magnetozones BIT1n–BIT5n may correspond as a whole to Newark magnetozones E20–E23. In particular, the T–J boundary interval at Italcementi Quarry, marked by a negative carbon isotope excursion and palynological turnover event (Galli et al., 2005; 2007), may correspond to the T–J palynological turnover event and associated spike in fern spore abundance occurring in the Newark basin a few meters above short (<30 ky) reverse magnetozone E23r. This magnetozone may incidentally correspond to the one-sample-based reverse interval BIT5n.1r within the uppermost part of the ZU3c subunit (Fig. 11). The thick normal polarity zone BIT5n at Italcementi Quarry may then correspond to the relatively long magnetozone E23n in the Newark APTS, and the interval from BIT4r to BIT2r to Newark magnetozones E22r–E21r. Continuing down section, the thick normal polarity magnetozone BIT2n at Brumano may correspond to E21n, implying an apparent abrupt increase in average sediment accumulation rates within the (faulted) ZU2 member at Brumano; this inference is supported by the facies (shallow-water carbonates with coral patch reefs) characterizing the ZU2 member and by an overall decrease of the NRM intensity consistent with dilution of the magnetic fraction within these sediments (Figs. 3 and 11). Below these levels, correlations are less clear and may involve the matching of the relatively thin magnetozone BIT1r with the relatively long Newark magnetozone E20r.

This correlation framework is used to construct a composite lithostratigraphic and magnetic polarity sequence for the Brumano and Italcementi Quarry sections encompassing a total of ~520 m of strata of Late Triassic–earliest Jurassic age, ~490 m of which is attributed to the Rhaetian as comprised between the first occurrence of *Misikella posthernsteini* and the end-Triassic extinction level at the base of the Malanotte Formation (Fig. 12). Average sediment accumulation rates based on this correlation framework generally vary between ~85 and ~170 m/Myr with inferred minima of ~20 m/Myr, corresponding to BIT1r and similar low values in

Table 1
Paleomagnetic directions and poles from Brumano and Italcementi Quarry.

			In situ				Tilt corrected						
Site	Comp.	*n*/*N*	*k*	α_{95}	Dec.	Inc.	*k*	α_{95}	Dec.	Inc.	Long./Lat.	A95	*K*
Brumano	A	175/145	60	1.5	356.5	61.2	56	1.6	347.6	42.1			
Brumano	Ch	175/116	20	3.0	359.5	44.3	18	3.2	353.5	27.8	201.9/58.9	3.0	20
Italcementi	A	162/118	22	2.8	4.4	62.3	19	3.1	291.4	62.9			
Italcementi	Ch	162/93	13.5	4.2	3.5	22.1	13	4.3	345.2	38.1	220.3/63.4	4.6	11

Site = sampling site (Brumano: 45.8°N, 9.5°E; Italcementi Quarry: 45.8°N, 9.4°E). Comp. = paleomagnetic component: A is recent overprint, Ch is characteristic component; *n*/*N* = number of specimens analyzed/number of specimens used to calculate the mean paleomagnetic directions and poles; *k* = Fisher precision parameter of the mean paleomagnetic direction; α_{95} = Fisher angle of half cone of 95% confidence about the mean paleomagnetic direction, in °; Dec. and Inc. = Declination (°E) and Inclination (°) of the mean paleomagnetic direction; Long./Lat. = Longitude (°E) and Latitude (°N) of the mean paleomagnetic pole; A95 = Fisher angle of half cone of 95% confidence about the mean paleomagnetic pole, in °; *K* = Fisher precision parameter of the mean paleomagnetic pole. Mean bedding attitude (azimuth of dip/dip) is 330°E/20° at Brumano and 236°E/43° at Italcementi Quarry.

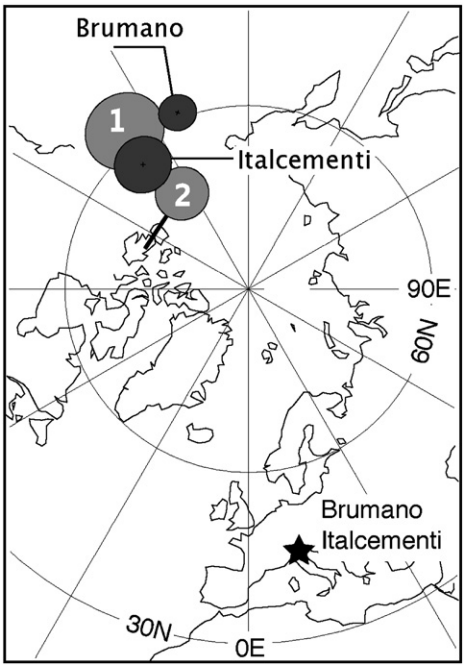

Fig. 10. Paleomagnetic poles calculated from the characteristic C component at Brumano and Italcementi Quarry (Table 1) compared to the Triassic paleomagnetic poles of NW Africa–Adria (Muttoni et al., 2001a; Table 3; entry #1: Middle–early Late Triassic; #2: Late Triassic–Early Jurassic). Equal-area projection was made with PaleoMac (Cogné, 2003). See text for discussion.

correspondence to BIT4n, which is however bracketed between faults (Fig. 12).

6. The Norian–Rhaetian boundary and the duration of the Rhaetian stage

Our age model implies that the lowermost occurrence of *Misikella posthernsteini*, whose first appearance is used here to define the base of the Rhaetian, should correspond to Newark levels older than E20n at ~207 Ma (Fig. 11). To further constrain the position of this bioevent in the Newark APTS, we take into account magneto-biostratigraphic data from the ~430 m thick Carnian–Norian Pizzo Mondello section from Sicily, which was correlated using a statistical approach to Newark magnetozones E5–E17 (correlation option #2 of Muttoni et al. (2004)) (Fig. 1). In general, this correlation option has two main implications: (i) the Carnian–Norian boundary (not yet formally decided by the Triassic sub-commission of the ICS), as recently proposed to fall at the first occurrence of *Metapolygnathus echinatus* and *Metapolygnathus parvus* within Pizzo Mondello magnetozone PM4r (Nicora et al., 2007), should correspond to Newark magnetozone E7, and (ii) Pizzo Mondello strata of Sevatian (late Norian) age with (among others) *Epigondolella bidentata* (Gullo, 1996) should broadly correspond to Newark magnetozones ~E15–E17n (Fig. 1). At Pizzo Mondello, Sevatian strata are conformably overlain (although a hiatus cannot be excluded) by a few tens of meters of early to middle Rhaetian calcilutites and marls (Portella Gebbia Formation), which are disconformably overlain by Jurassic sediments (Gullo, 1996; Muttoni et al., 2004) (Figs. 1 and 11). The Portella Gebbia Formation, poorly exposed and thus not sampled for magnetostratigraphy (Muttoni et al., 2004), records at its base the first occurrence of *M. posthernsteini* (Gullo, 1996; Muttoni et al., 2004) (Fig. 11).

Considering that first occurrence of *Misikella posthernsteini* was recovered ~120 m below the oldest proved magnetozone BIT1n at Brumano, which is possibly correlative to Newark magnetozone E20n, whereas at Pizzo Mondello this biodatum was recovered in strata again with no magnetostratigraphic control but overlying magnetozone PM12n, which corresponds to E17n, we conclude that the position of the Norian–Rhaetian boundary (as defined by the first appearance of *M. posthernsteini*) should conservatively fall within Newark magnetozones E17r–E19r in the ~207–210 Ma time interval (Fig. 11). This would be in basic agreement with the original position indicated by Kent et al. (1995) and Kent and Olsen (1999) using pollen biostratigraphy, i.e. magnetozone E18 at 208–209 Ma.

Further refinements of this chronostratigraphic position involving the use of additional sections from the literature are at present difficult to achieve. For example, at St. Audrie's Bay in Britain, *Misikella posthernsteini* was not recorded (Hounslow et al., 2004). The ~9 m thick Steinbergkogel STKB + C section from Austria, containing toward its base the presumed first appearance of *M. posthernsteini*, bears largely reverse magnetic polarity and shows little magnetostratigraphic resemblance with the nearby ~4 m thick Steinbergkogel STK-A section, a candidate GSSP for the base of the Rhaetian (defined by the first appearance of *M. posthernsteini*; Krystyn et al., 2007a). In the ~30 m thick Oyuklu section from Turkey (Gallet et al., 2007), *M. posthernsteini* occurs broadly from the (faulted) section base to section top across strata dominated by normal magnetic polarity showing little visual matching with the presumably coeval Steinbergkogel STKB + C section of mainly reverse polarity. In summary, there is no unique magnetostratigraphic correlation between the supposedly coeval but highly condensed Steinbergkogel STKB + C, Steinbergkogel STK-A, and Oyuklu sections (*contra* Krystyn et al., 2007b), or between Oyuklu and Pizzo Mondello (*contra* Gallet et al., 2007), or between Steinbergkogel or Oyuklu and the Brumano and Italcementi Quarry sections of this study, suggesting that these very thin and evidently highly condensed sections have significant cryptic internal hiatuses. For further discussion, we refer to the review of Triassic magnetostratigraphic correlations by Hounslow and Muttoni (in press), with the note of caution that additional work is required to sort out correlations of Rhaetian sections.

For estimating the duration of the Rhaetian, we assume a Triassic–Jurassic boundary interval time horizon that is equivalent to the palynological extinction level placed in the Newark APTS at 202 Ma immediately above Newark magnetozone E23r and immediately below the first CAMP lavas (e.g., Kent and Olsen, 1999); recent ages obtained from the North Mountain Basalt (Schoene et al., 2006), which appears to be the northward equivalent of the oldest basalts in the Newark basin (Olsen et al., 2003; Whiteside et al., 2007) and similarly overlies the end-Triassic palynofloral extinction horizon, suggest that the numeric date may be closer to 201.5 Ma, which would simply shift the Newark APTS (Kent and Olsen, 1999) that was pegged to this dated horizon. For the older bounding age, we assume that the Norian–Rhaetian boundary can be correlated to Newark magnetozones E17r–E19r in the ~207–210 Ma interval (or E18 at 208–209 Ma according to Newark palynostratigraphy; e.g., Kent and Olsen, 1999); accordingly, the duration of the Rhaetian is on the order of ~5.5–8.5 Myr (Fig. 13, left). The Rhaetian would be even somewhat

Fig. 11. Magnetostratigraphic correlation of the Brumano and Italcementi Quarry sections from magnetozones BIT1n to BIT5n to the upper part of the Pizzo Mondello section (Muttoni et al., 2004) and the Newark APTS (Kent et al., 1995; Kent and Olsen, 1999; Olsen and Kent, 1999). Relative sedimentation rates are inferred from the NRM values at Brumano (Fig. 3), and from the IRM values at Italcementi Quarry (Fig. 4) whereby the higher the NRM or IRM, the lower the sedimentation rate (see text for details). The carbon isotope profile with negative excursion at the Triassic–Jurassic boundary is from the Malanotte section located a few hundred meters to the SE of the Italcementi Quarry section (Galli et al., 2005; 2007). The first occurrence of *Misikella posthernsteini*, a marker of the Norian–Rhaetian boundary, has been reported about 120 m below basal magnetozone BIT1n (see Fig. 3). Lithology symbols as in Figs. 2 and 3. Malan. is Malanotte Formation; RSS is Riva di Solto Shale.

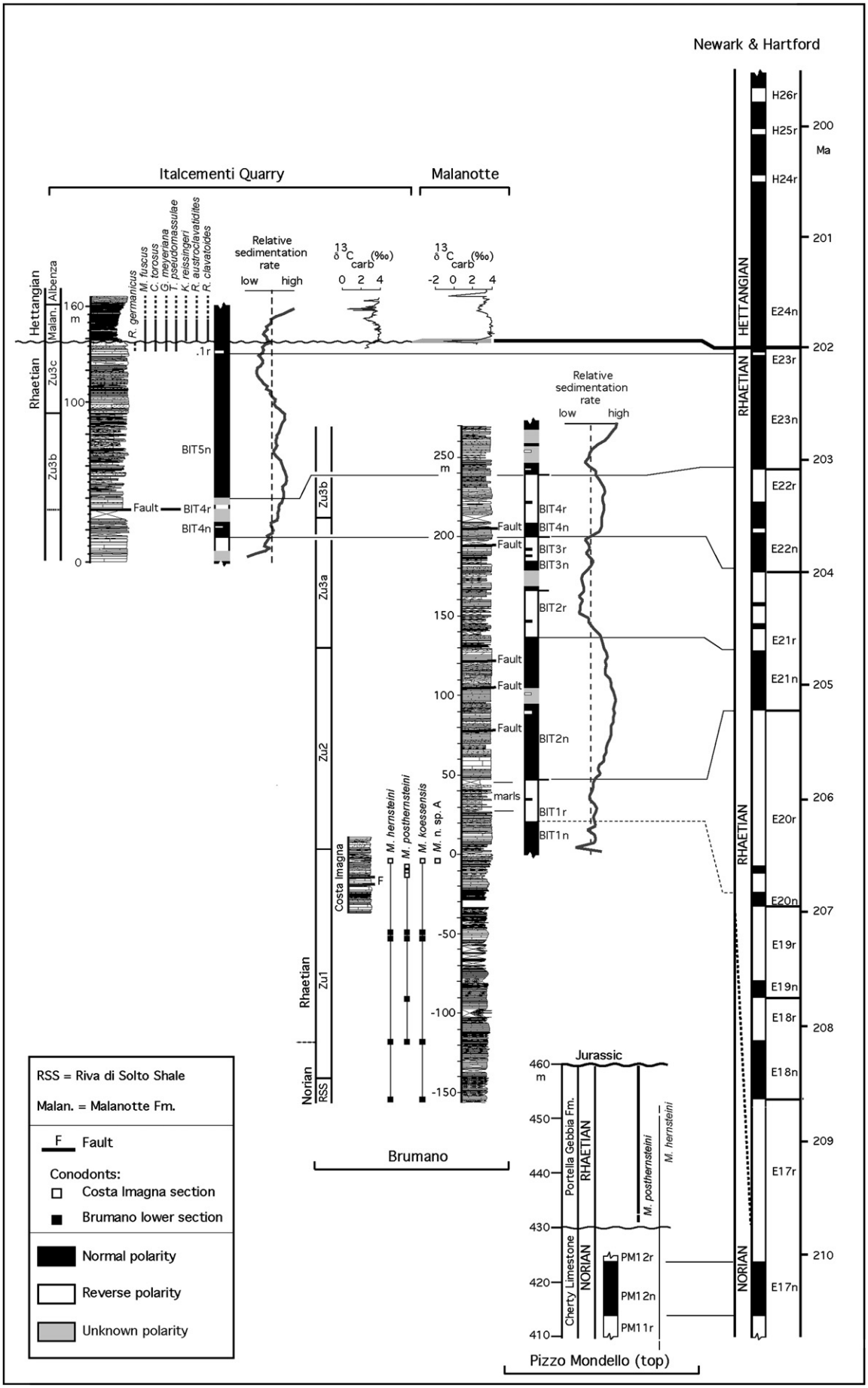
Newark & Hartford
Italcementi Quarry
Malanotte
Brumano
Pizzo Mondello (top)
Hettangian
Rhaetian
Malan.
Albenza
Zu3c
Zu3b
Zu3a
Zu2
Zu1
Norian
RSS
Costa Imagna
R. germanicus
M. tuscus
C. torosus
G. meyeriana
G. pseudomassulae
K. ressingeri
R. austrocla vatidites
R. clavatoides
Relative sedimentation rate
low high
δ13Ccarb (‰)
BIT5n
BIT4r
BIT4n
BIT3r
BIT3n
BIT2r
BIT2n
BIT1r
BIT1n
Fault
marls
M. hernsteini
M. posthernsteini
M. koessensis
M. n. sp. A
Jurassic
Portella Gebbia Fm.
Cherty Limestone
RHAETIAN
NORIAN
PM12r
PM12n
PM11r
HETTANGIAN
H26r
H25r
H24r
E24n
E23r
E23n
E22r
E22n
E21r
E21n
E20r
E20n
E19r
E19n
E18r
E18n
E17r
E17n
Ma
RSS = Riva di Solto Shale
Malan. = Malanotte Fm.
F Fault
Conodonts:
Costa Imagna section
Brumano lower section
Normal polarity
Reverse polarity
Unknown polarity

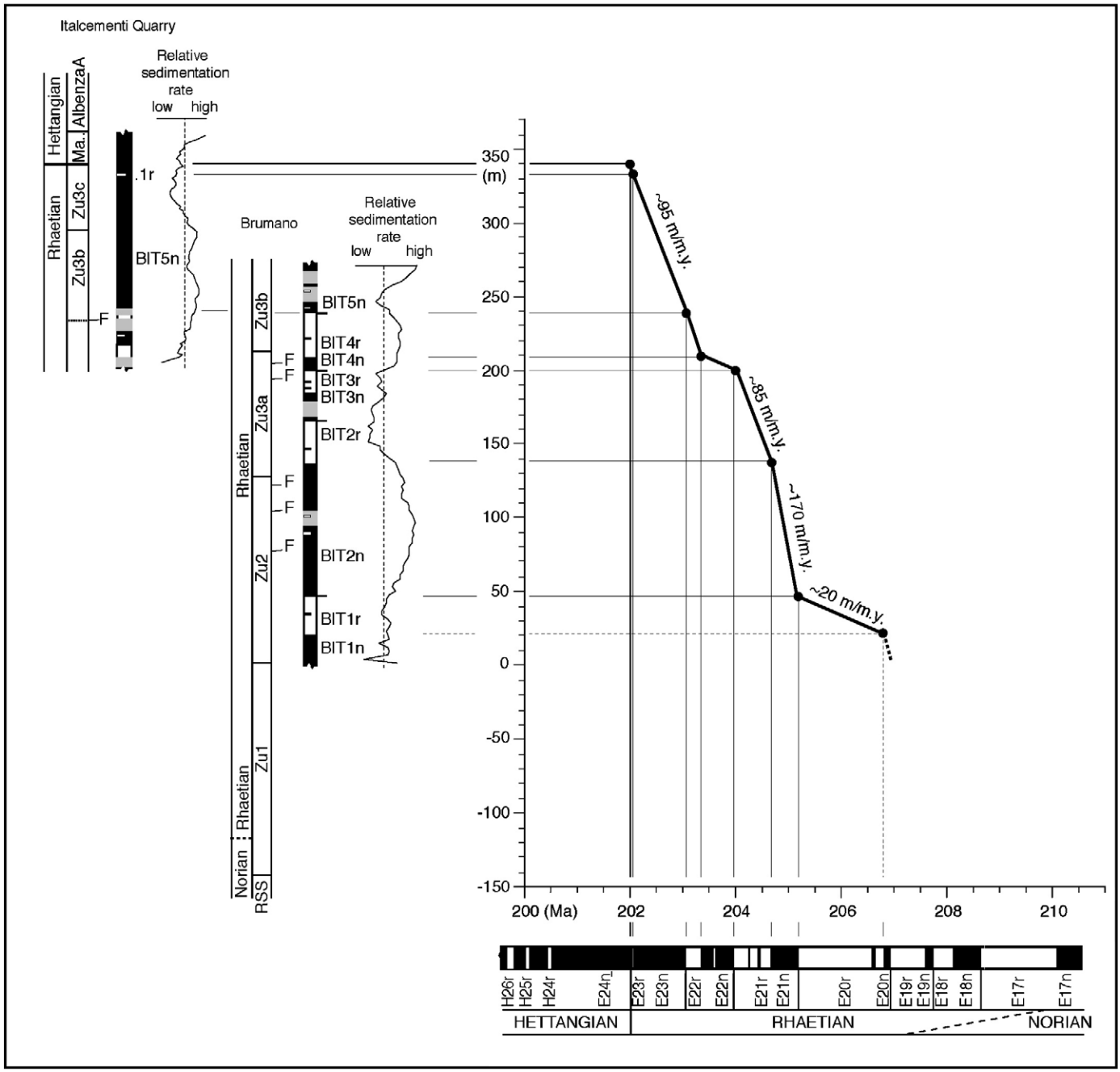

Fig. 12. Age model of sedimentation at Brumano and Italcementi Quarry obtained by means of correlation to the Newark APTS. Relative sedimentation rate curves are described in caption to Fig. 11 and in the text. Ma. is Malanotte Formation; RSS is Riva di Solto Shale.

longer if the T–J boundary was instead placed, as proposed by Hillebrandt et al. (2007), at the first occurrence of *Psiloceras spelae* in the 25 m thick Kuhjoch section.

This solution largely contrasts with a much shorter duration of the Rhaetian in alternative Late Triassic magneto-biostratigraphic schemes from the literature. For example, Carnian–Norian data from Kavaalani (Gallet et al., 2000), Kavur Tepe (Gallet et al., 1993), Pizzo Mondello (lower part; Muttoni et al., 2001b), Bolücektasi Tepe (Gallet et al., 1992), and Scheiblkogel (Gallet et al., 1996) were used by Krystyn et al. (2002) to construct a Tethyan composite magneto-biostratigraphic sequence that assumed biozones of equal duration; this composite was correlated to Newark magnetozones E3–E22 and used to infer a duration of the Rhaetian (not sampled) of only ~2 Myr and encompassing only ~4 magnetozones. More recently, Gallet et al. (2007) correlated data from Oyuklu, Pizzo Mondello (upper part; Muttoni et al., 2004), and the Tethyan composite sequence of Gallet et al. (2003) to the Newark APTS and inferred a duration of the Rhaetian of ~2 Myr while proposing that the Rhaetian is in part missing in the Newark sequence, whereby Rhaetian magnetozones from Oyuklu would be largely equivalent to a cryptic hiatus between the top of the Passaic Formation and the CAMP basalts in the Newark section. We contend that piecing together a magnetic polarity sequence from condensed sections punctuated by stratigraphic gaps is likely to produce a distorted polarity pattern and more problematical correlations to the standard Newark APTS. For example, middle Norian (Alaunian) magnetozones in the composite magneto-biostratigraphic sequence of Krystyn et al. (2002) may encompass Newark magnetozones ~E13–E15 rather than ~E13–E17 so that the overlying Sevatian magnetozones may correlate to Newark levels at and immediately above E15 rather than at and above E17 as proposed by Krystyn et al. (2002), thus supporting the existence of a long Rhaetian.

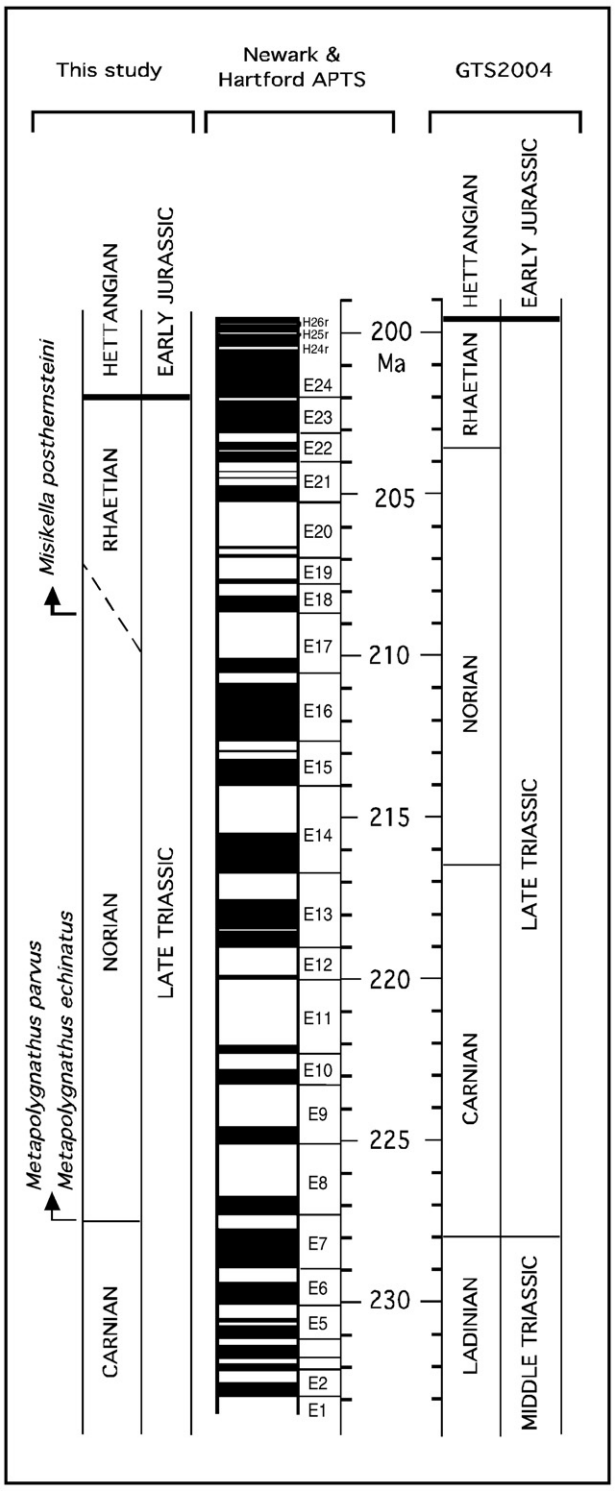

Fig. 13. The Triassic chronostratigraphy from this study compared to the Newark and Hartford basin astronomical polarity time scale (APTS) and the recent Triassic time scale of Gradstein et al. (2004). See text for discussion.

7. Conclusions

We obtained an estimate for the duration of the Rhaetian of ~5.5–8.5 Myr by taking into account new magneto-biostratigraphic data from the ~520 m thick Brumano and Italcementi Quarry sections near Bergamo as well as the upper portion of the ~430 m thick Pizzo Mondello section from Sicily (Muttoni et al., 2004) and their correlations to the Newark APTS. Despite the admitted correlation uncertainties, the relevant conclusion of this study is that there are at least 490 m of Rhaetian strata bearing *Misikella posthernsteini* and bracketing significantly more magnetic polarity zones and, by inference, more time sampled than recognized in previously described thinner and apparently more condensed sections from the literature, suggesting the existence of a long rather than a short Rhaetian.

Acknowledgements

Helpful comments by Mark W. Hounslow and an anonymous reviewer greatly improved the manuscript. Olsen and Kent were partially supported in this work by NSF EAR-07-53496. This is Lamont-Doherty contribution #0000.

References

Brack, P., Rieber, H., Nicora, A., Mundil, R., 2005. The Global Boundary Stratotype Section and Point (GSSP) of the Ladinian Stage (Middle Triassic) at Bagolino (Southern Alps, Northern Italy) and its implications for the Triassic time scale. Episodes 28 (4), 233–244.

Cogné, J.P., 2003. PaleoMac: a Macintosh™ application for treating paleomagnetic data and making plate reconstructions. Geochemistry, Geophysics, Geosystems 41 (1), 1007.

Channell, J.E.T., Kozur, H.W., Sievers, T., Mock, R., Aubrecht, R., 2003. Carnian–Norian biomagnetostratigraphy at Silická Brezová (Slovakia): correlation to other Tethyan sections and to the Newark Basin. Palaeogeography, Palaeoclimatology, Palaeoecology 191, 65–109.

Doglioni, C., Bosellini, A., 1987. Eoalpine and mesoalpine tectonics in the Southern Alps. Geologische Rundschau 76 (3), 735–754.

Gallet, Y., Besse, J., Krystyn, L., Marcoux, J., Theveniaut, H., 1992. Magnetostratigraphy of the Late Triassic Bolücektasi Tepe section (southwestern Turkey): implications for changes in magnetic reversal frequency. Physics of the Earth and Planetary Interiors 73, 85–108.

Gallet, Y., Besse, J., Krystyn, L., Theveniaut, H., Marcoux, J., 1993. Magnetostratigraphy of the Kavur Tepe section (southwestern Turkey): a magnetic polarity time scale for the Norian. Earth and Planetary Science Letters 117, 443–456.

Gallet, Y., Besse, J., Krystyn, L., Marcoux, J., 1996. Norian magnetostratigraphy from the Scheiblkogel section, Austria: constraint on the origin of the Antalya Nappes, Turkey. Earth and Planetary Science Letters 140, 113–122.

Gallet, Y., Besse, J., Krystyn, L., Marcoux, J., Guex, J., Theveniaut, H., 2000. Magnetostratigraphy of the Kavaalani section (southwestern Turkey): consequence for the origin of the Antalya Calcareous Nappes (Turkey) and for the Norian (Late Triassic) magnetic polarity timescale. Geophysical Research Letters 27, 2033–2036.

Gallet, Y., Krystyn, L., Besse, J., Marcoux, J., 2003. Improving the Upper Triassic numerical time scale from cross-correlation between Tethyan marine sections and the continental Newark basin sequence. Earth and Planetary Science Letters 212, 255–261.

Gallet, Y., Krystyn, L., Marcoux, J., Besse, J., 2007. New constraints on the End-Triassic (Upper Norian–Rhaetian) magnetostratigraphy. Earth and Planetary Science Letters 255, 458–470.

Galli, M.T., Jadoul, F., Bernasconi, S.M., Weissert, H., 2005. Anomalies in global carbon cycling at the Triassic/Jurassic boundary: evidence from a marine C-isotope record. Palaeogeography, Palaeoclimatology, Palaeoecology 216, 203–214.

Galli, M.T., Jadoul, F., Bernasconi, S.M., Cirilli, S., Weissert, H., 2007. Stratigraphy and palaeoenvironmental analysis of the Triassic–Jurassic transition in the western Southern Alps (Northern Italy). Palaeogeography, Palaeoclimatology, Palaeoecology 244, 52–70.

Gradstein, F.M., Ogg, J.G., Smith, A.G., 2004. A Geologic Time Scale 2004. Cambridge University Press.

Gullo, M., 1996. Conodont biostratigraphy of uppermost Triassic deep-water calcilutites from Pizzo Mondello (Sicani Mountains): evidence for Rhaetian pelagites in Sicily. Palaeogeography, Palaeoclimatology, Palaeoecology 126, 309–323.

Hillebrandt von, A., Krystyn, L., Kuerschner, W.M., Bown, P.R., McRoberts, C., Ruhl, M., Simms, M., Tomasovych, A., Urlichs, M., 2007. A candidate GSSP for the base of the Jurassic in the Northern Calcareous Alps (Kuhjoch section, Karwendel Mountains, Tyrol, Austria). International Subcommission of Jurassic Stratigraphy Newsletter 34, 2–20.

Hounslow, M.W. and Muttoni, G., in press. The geomagnetic polarity timescale for the Triassic: linkage to stage boundary definitions. In: S.G. Lucas (Editor), The Triassic Time Scale. Geological Society, London, Special Publication.

Hounslow, M.W., Posen, P.E., Warrington, G., 2004. Magnetostratigraphy and biostratigraphy of the Upper Triassic and lowermost Jurassic succession, St. Audrie's Bay, UK. Palaeogeography, Palaeoclimatology, Palaeoecology 213, 331–358.

Jadoul, F., Galli, M.T., 2008. The Hettangian shallow water carbonates after the Triassic/Jurassic biocalcification crisis. Rivista Italiana di Paleontologia e Stratigrafia 114, 453–470.

Kent, D.V., Olsen, P.E., 1999. Astronomically tuned geomagnetic polarity time scale for the Late Triassic. Journal of Geophysical Research 104, 12,831–12,841.

Kent, D.V., Muttoni, G., 2003. Mobility of Pangea: Implications for Late Paleozoic and Early Mesozoic paleoclimate. In: LeTourneau, P.M., Olsen, P.E. (Eds.), The Great Rift Valleys of Pangea in Eastern North America. : Tectonics, Structure, and Volcanism, vol. 1. Columbia University Press, New York, pp. 11–20.

Kent, D.V., Olsen, P.E., 2008. Early Jurassic magnetostratigraphy and paleolatitudes from the Hartford continental rift basin (eastern North America): testing for polarity bias and abrupt polar wander in association with the central Atlantic magmatic province. Journal of Geophysical Research 113, B06105. doi:10.1029/2007JB005407.

Kent, D.V., Olsen, P.E., Witte, W.K., 1995. Late Triassic–earliest Jurassic geomagnetic polarity sequence and paleolatitudes from drill cores in the Newark rift basin, eastern North America. Journal of Geophysical Research 100, 14,965–14,998.

Kent, D.V., Muttoni, G., Brack, P., 2006. Reply to 'Discussion of "Magnetostratigraphic confirmation of a much faster tempo for sea-level change for the Middle Triassic Latemar platform carbonates" by D. V. Kent, G. Muttoni and P. Brack [Earth Planet. Sci. Lett., 228 (2004): 369–377]' by L. Hinnov: Earth and Planetary Science Letters, 243: 847–850.

Kozur, H., Mock, R., 1991. New Middle Carnian and Rhaetian Conodonts from Hungary and the Alps. Stratigraphic Importance and Tectonic Implications for the Buda Mountains and Adjacent Areas: Jb. Geol. B.-A., vol. 134/2, pp. 271–297.

Krystyn, L., 1987. Zur Rhaet-Stratigraphie in den Zlambach-Schichten (vorläufiger Bericht): Sitz. Ber. Akad. Wiss. Wien, math.-nat. Kl., vol. 196, pp. 21–36.

Krystyn, L., 1990. A Rhaetian stage — chronostratigraphy, subdivisions and their intercontinental correlation. Albertiana 8, 15–24.

Krystyn, L., Gallet, Y., Besse, J., Marcoux, J., 2002. Integrated Upper Carnian to Lower Norian biochronology and implications for the Upper Triassic magnetic polarity time scale. Earth and Planetary Science Letters 203, 343–351.

Krystyn, L., Bouquerel, H., Kuerschner, W., Richoz, S., Gallet, Y., 2007b. Proposal for a candidate GSSP for the base of the Rhaetian Stage. In: Lucas, S.G., Spielmann, J.A. (Eds.), The Global Triassic. New Mexico Museum of Natural History and Science Bulletin, pp. 189–199.

Krystyn, L., Richoz, S., Gallet, Y., Bouquerel, H., Kürschner, W.M., Spötl, C., 2007a. Updated bio- and magnetostratigraphy from Steinbergkogel (Austria), candidate GSSP for the base of the Rhaetian stage. Albertiana 36, 164–172.

Lowrie, W., 1990. Identification of ferromagnetic minerals in a rock by coercivity and unblocking temperature properties. Geophysical Research Letters 17, 159–162.

Mietto, P., Andreetta, R., Broglio Loriga, C., Buratti, N., Cirilli, S., De Zanche, V., Furin, S., Gianolla, P., Manfrin, S., Muttoni, G., Neri, C., Nicora, A., Posenato, R., Preto, N., Rigo, M., Roghi, G., Spötl, C., 2007. A Candidate Of The Global Boundary Stratotype Section And Point For The Base Of The Carnian Stage (Upper Triassic): GSSP at the base of the canadensis Subzone (FAD of Daxatina) in the Prati di Stuores/Stuores Wiesen section (Southern Alps, NE Italy). Albertiana 36, 78–97.

Morton, N., 2008a. Selection and voting procedures for the base Hettangian. International Subcommission on Jurassic Stratigraphy, Newsletter 35 (1), 67.

Morton, N., 2008b. Details of voting on proposed GSSP and ASSP for the base of the Hettangian Stage and Jurassic System. International Subcommission on Jurassic Stratigraphy, Newsletter 35 (1), 74.

Morton, N., Warrington, G., Bloos, G., 2008. Foreword. International Subcommission on Jurassic Stratigraphy, Newsletter 35 (1), 68–73.

Muttoni, G., Garzanti, E., Alfonsi, L., Cirilli, S., Germani, D., Lowrie, W., 2001a. Motion of Africa and Adria since the Permian: paleomagnetic and paleoclimatic constraints from northern Libya. Earth and Planetary Science Letters 192, 159–174.

Muttoni, G., Kent, D.V., Di Stefano, P., Gullo, M., Nicora, A., Tait, J., Lowrie, W., 2001b. Magnetostratigraphy and biostratigraphy of the Carnian/Norian boundary interval from the Pizzo Mondello section (Sicani Mountains, Sicily). Palaeogeography, Palaeoclimatology, Palaeoecology 166, 383–399.

Muttoni, G., Kent, D.V., Olsen, P.E., Di Stefano, P., Lowrie, W., Bernasconi, S., Martín Hernández, F., 2004. Tethyan magnetostratigrapy from Pizzo Mondello and correlation to the Late Triassic Newark APTS. Geological Society of America Bulletin 116, 1043–1058.

Nicora, A., Balini, M., Bellanca, A., Bertinelli, A., Bowring, S.A., Di Stefano, P., Dumitrica, P., Guaiumi, C., Gullo, M., Hungerbuehler, A., Levera, M., Mazza, M., McRoberts, C.A., Muttoni, G., Preto, N., Rigo, M., 2007. The Carnian/Norian boundary interval at Pizzo Mondello (Sicani Mountains, Sicily) and its bearing for the defnition of the GSSP of the Norian Stage. Albertiana 36, 102–115.

Olsen, P.E., Kent, D.V., 1999. Long-period Milankovitch cycles from the Late Triassic and Early Jurassic of eastern North America and their implications for the calibration of the Early Mesozoic time-scale and the long-term behaviour of the planets. Philosophical Transactions of the Royal Society of London, Series A 357, 1761–1786.

Olsen, P.E., Kent, D.V., Cornet, B., Witte, W.K., Schlische, R.W., 1996. High-resolution stratigraphy of the Newark rift basin (early Mesozoic, eastern North America). Geological Society of America Bulletin 108, 40–77.

Olsen, P.E., Kent, D.V., Et-Touhami, M., Puffer, J., 2003. Cyclo-, magneto-, and biostratigraphic constraints on the duration of the CAMP event and its relationship to the Triassic–Jurassic boundary. In: Hames, W.E., McHone, J.G., Renne, P.R., Ruppel, C. (Eds.), Central Atlantic Magmatic Province. Geophysical Monograph, vol. 136. American Geophysical Union, pp. 7–32.

Pálfy, J., Demény, A., Haas, J., Carter, E.S., Görög, A., Halász, D., Oravecz-Scheffer, A., Hetényi, M., Márton, E., Orchard, M.J., Ozsvárt, P., Vetö, I., Zajzon, N., 2007. Triassic–Jurassic boundary events inferred from integrated stratigraphy of the Csővár section, Hungary. Palaeogeography, Palaeoclimatology, Palaeoecology 244, 11–33.

Schoene, B., Crowley, J.L., Condon, D.J., Schmitz, M.D., Bowring, S.A., 2006. Reassessing the uranium decay constants for geochronology using ID-TIMS U–Pb data. Geochimica et Cosmochimica Acta 70, 426–445.

Tauxe, L., Kent, D.V., 2004. A simplified statistical model for the geomagnetic field and the detection of shallow bias in palaeomagnetic inclinations: was the ancient magnetic field dipolar? In: Channell, J.E.T., Kent, D.V., Lowrie, W., Meert, J.G. (Eds.), Timescales of the Palaeomagnetic Field. Geophysical Monograph, vol. 145. American Geophysical Union, pp. 101–116.

Whiteside, J.H., Olsen, P.E., Kent, D.V., Fowell, S.J., Et-Touhami, M., 2007. Synchrony between the Central Atlantic magmatic province and the Triassic–Jurassic mass-extinction event? Palaeogeography, Palaeoclimatology, Palaeoecology 244, 345–367.

Yin, H., Zhang, K., Tong, J., Yang, Z., Wu, S., 2001. The Global Stratotype Section and Point (GSSP) of the Permian–Triassic Boundary. Episodes 24, 102–114.